Available online at www.sciencedirect.com
ScienceDirect
Advances in Space Research 48 (2011) 1848–1857
ADVANCES IN SPACE RESEARCH (a COSPAR publication)
www.elsevier.com/locate/asr

Numerical techniques for generating and refining solar sail trajectories

Geoffrey G. Wawrzyniak, Kathleen C. Howell *

School of Aeronautics and Astronautics, Armstrong Hall of Engineering, 701 West Stadium Avenue, West Lafayette, IN 47907-2045, USA

Available online 19 April 2011

Abstract

Like all applications in trajectory design, the design of solar sail trajectories requires a transition from analytical models to numerically generated realizations of an orbit. In astrodynamics, three numerical strategies are often employed. Differential correctors (also known as shooting methods) are perhaps the most common techniques. Finite-difference methods and collocation schemes are also employed and are successful in generating trajectories with pseudo-continuous control histories. These three numerical techniques are employed here to generate periodic trajectories displaced below the Moon in a circular restricted three-body system. All these approaches reveal trajectory options within the design space for solar sail applications.

Keywords: Solar sails; Shooting; Differential correctors; Finite-difference method; Collocation

1. Introduction

Generating spacecraft trajectories in multi-body regimes to meet mission requirements is not easy. Generating *solar sail* trajectories in multi-body regimes is even more challenging. Trajectory design for any spacecraft mission application typically involves either well-developed analytical approximations or linearization relative to a known solution. These approximations are typically based on well-understood dynamics. However, when two or more large bodies (e.g., Earth and Moon, or Sun, Earth, and Moon) are present, trajectories in a multi-body gravitational environment can become chaotic. The problem is further complicated when the additional force from a solar sail is incorporated.

Various authors have recently demonstrated that a solar sail spacecraft can potentially support a communications architecture for an outpost at the lunar south pole (LSP) (Ozimek et al., 2009, 2010; Wawrzyniak and Howell, in press; Simo and McInnes, 2010). These analyses are usually formulated within an Earth–Moon circular restricted three-body (EM-CR3B) model. Working within this model (as opposed to a Moon-centered, inertial model, for example) has the advantages of (1) connecting solar sail orbits to solutions associated with the five classical Lagrange points, (2) including the two primary gravitational bodies that affect a trajectory in view of the LSP, and (3) supplying an easily understood geometry with respect to a "fixed" Earth and Moon. Concerning the third purpose for an Earth–Moon model, note that the Moon is tidally locked to the Earth, and a base on the Moon is essentially stationary in an EM-CR3B system. Working within a frame fixed to the Earth and the Moon, however, poses new challenges for solar sail mission design because the Sun moves with respect to a fixed Earth and Moon and the system dynamics in a multi-body environment, and including a solar sail, are complex. Current analytical tools are not sufficiently developed to reveal more than a few desired, or even viable, solutions.

Certainly, analytical perturbation approaches are available for solar sail trajectory design in two- and three-body regimes, and in frames where the Sun is either stationary or moving. However, recent work using numerical techniques for solving boundary value problems (BVPs) shows promise for uncovering solutions for spacecraft trajectory design involving solar sails (Ozimek et al., 2009, 2010;

* Corresponding author. Tel.: +1 765 494 5786; fax: +1 765 494 0307.
E-mail addresses: gwawrzyn@purdue.edu (G.G. Wawrzyniak), howell@purdue.edu (K.C. Howell).

0273-1177/$36.00 © 2011 COSPAR. Published by Elsevier Ltd. All rights reserved.
doi:10.1016/j.asr.2011.04.012

Wawrzyniak and Howell, in press). Numerical strategies for solving BVPs, such as shooting (or differential-corrections processes), finite-difference methods, as well as collocation, greatly expand the range of the available design space for trajectories in unstable, nonlinear, or chaotic dynamical systems. Shooting and collocation methods are often incorporated into trajectory optimization schemes, which are formulated as boundary value problems (Betts, 1998; Rao, 2009). Some numerical methods, such as collocation and finite-difference methods, require little knowledge of the complicated dynamical structure to initiate the process. Furthermore, new mission opportunities, options not deduced via analytical techniques, may emerge.

A brief description of the behavior of solar sail spacecraft in the EM system is first introduced. An overview of the differential corrections processes for solar sail trajectories is followed by a discussion of finite-difference methods, then collocation strategies. Other numerical tools for generating orbits do exist, but are left for future investigations. While these numerical procedures may be employed as part of an optimization scheme, optimization is not discussed here. Finally, some examples using the solution from one technique to initialize a different strategy are summarized.

2. Dynamical model

The vector equations of motion for an idealized solar sail spacecraft in a CR3B system and located approximately one AU from the Sun are formulated in terms of coordinates rotating relative an inertial frame and appear as

$$\ddot{\mathbf{r}} + 2\boldsymbol{\omega} \times \dot{\mathbf{r}} + \nabla U - \frac{a_0}{a^*}(\hat{\ell}(t) \cdot \mathbf{u})^2 \mathbf{u} = 0 \tag{1}$$

where ∇U is the gradient of a pseudo-potential that includes the centripetal acceleration and the gravity effects of the two primaries.[1] The final term in Eq. (1) represents the acceleration of the sail, non-dimensionalized by the system acceleration, a^* (2.73 mm/s^2 for the EM system); a_0 is the sail's characteristic acceleration at one AU, $\hat{\ell}(t)$ is the sunlight direction, and $\mathbf{u}$ is the direction of the sailface normal. The angle between the sail normal and the sun-line is commonly denoted α, and equals $\cos^{-1}(\hat{\ell}(t) \cdot \mathbf{u})$. The Sun moves about the EM system at a rate of Ω, that is, the ratio of the synodic rate to the sidereal rate (approximately 0.925), and, thus,

$$\hat{\ell}(t) = \cos \Omega t \hat{\mathbf{x}} - \sin \Omega t \hat{\mathbf{y}} + 0\hat{\mathbf{z}} \tag{2}$$

as expressed in the EM rotating frame. The EM-system model is illustrated in Fig. 1. The Sun is assumed to be infinitely far from the system such that solar gravity is negligible and the rays of sunlight are parallel. Note that while solar gravity is not included in this model, neither is lunar-orbit eccentricity, which may have a greater effect on the accuracy of the solutions from the CR3B model. A higher fidelity model will improve the accuracy of the solutions. Regardless of whether the equations of motion describe a four-body model (Farquhar and Kamel, 1970; Andreu, 1998; Guzmán, 2001) or an ephemeris model, the numerical methods should be adaptable to the choice of model. Ozimek et al. (2009) successfully adapt a collocation scheme for the LSP problem to an ephemeris model, and Grebow et al. (2010) apply a collocation routine for the LSP problem for a spacecraft that employs electric propulsion.

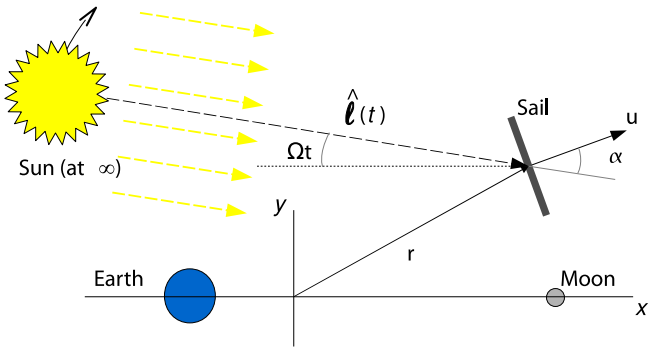

Fig. 1. EM system model.

In applications where the Sun and the Earth are the primaries (e.g., SE-CR3B model, where $a^* = 5.93$ mm/s^2), $\hat{\ell}$ is stationary within the reference frame and parallel to the Sun–sail vector. Surfaces of stationary points, or equilibrium surfaces, exist in the SE-CR3B system and supply a large solution space from which orbits may be developed using analytical techniques (McInnes et al., 1994). In the EM system, instantaneous surfaces can be computed because the Sun moves with respect to the frame and the acceleration from the sail is time-variant (McInnes et al., 1994). Equilibria do exist when $\alpha = 90°$ or $a_0 = 0$; then, the five classical Lagrange points are the equilibrium points. Nevertheless, periodic orbits do exist in the EM system and are examined in the following sections.

3. Differential correctors (shooting)

Shooting methods, often termed differential corrections (DC) processes, are common tools for generating trajectories in astrodynamics. In general, some sort of approximation is developed via analytical techniques that incorporate knowledge of the system dynamics. Often, a trajectory is approximated via a linearization process relative to a known reference solution to the nonlinear differential equations, such as an equilibrium point. States from this approximation are used to initialize numerical integration of the nonlinear equations of motion. A state transition matrix (STM) is propagated along with a six-state (position and velocity) trajectory and is used to linearly correct the states and, thus, select the initial values of the elements. Dynamical characteristics extracted from the STM are

[1] Vectors are denoted in boldface. Unit vectors are denoted with hats (e.g., "$\hat{\mathbf{x}}$"). Note that $\mathbf{u} \equiv \hat{\mathbf{u}}$.

effective at describing the consequences of small perturbations and, as a result, DC is a popular tool for generating, or updating, numerical representations of orbits. Shooting methods are often described in terms of two types: (1) single shooting and (2) multiple shooting. In single shooting, a single arc is defined from an initial point to a final target. Multiple shooting (Stoer and Bulirsch, 2002) and two-level correctors (Howell and Pernicka, 1988) exploit short arc segments, usually along non-periodic orbits, for a more stable numerical process; path constraints (e.g., elevation) and continuity between arc segments are enforced at the endpoints along each segment. The sail attitude is generally fixed along each arc segment (or the entire orbit if single shooting is employed).

Nuss (1998) and McInnes (2000) both use single-shooting methods to generate halo orbits in the SE-CR3B regime. Nuss begins with a third-order approximation for a halo orbit in the vicinity of a collinear Lagrange point (L_1). Nuss uses shooting to deliver a nonlinear solution, and then applies continuation based on a_0 to extend the nonlinear, solar sail halo orbits toward the Sun (Nuss, 1998). McInnes expands the approximation to include solar sail effects and generates families near artificial Lagrange points for various a_0 (McInnes, 2000). In Waters et al. (2007), a single-shooting DC process is employed to correct Lindstedt–Poincaré approximations of periodic orbits above the SE ecliptic plane. Likewise, Farrés et al. (2010) employ multiple shooting as a tool to compute periodic orbits near the Sun–Earth–Sail L_1 point. In each of the preceding examples, sail attitude is assumed to be fixed relative to the modeled frame.

As an example of the computation of a solar sail trajectory using shooting in the EM problem, a linear approximation for elliptical orbits that are shifted, and remain, below the Lagrange points and parallel to the EM orbit plane is detailed in Simo and McInnes (2010). In these orbits, the pitch angle, α, is fixed to supply a constant out-of-plane force; based on the linearized equations of motion, the pitch angle that supplies the maximum out-of-plane force is 35.264°. The orbits in Simo and McInnes (2010) are plotted directly from the approximation. To compute orbits that are periodic solutions to the *nonlinear* equations of motion, the Simo–McInnes approximation is used to seed a DC scheme here.

The process is developed to determine a family of periodic orbits in the nonlinear model. The initial state, as specified on the xz plane, from a linear approximation corresponding to an out-of-plane orbit in Simo and McInnes (2010) supplies an initial guess for a nonlinear trajectory that is corrected using the DC technique. An STM is constructed based on the variations of $\mathbf{r}$, $\dot{\mathbf{r}}$, and a_0 such that deviations at the beginning of the arc, $\{\delta\mathbf{r}_i\ \delta\dot{\mathbf{r}}_i\ \delta(a_0)\}$, are linearly mapped to some future time, $\{\delta\mathbf{r}_f\ \delta\dot{\mathbf{r}}_f\}$. Higher-order state transition formulations are available (Julier et al., 1995; Sengupta et al., 2007); however, STMs based on first-order variations and linear mappings are typically used for most trajectory-design applications. A deviation in $\mathbf{r}$ is computed

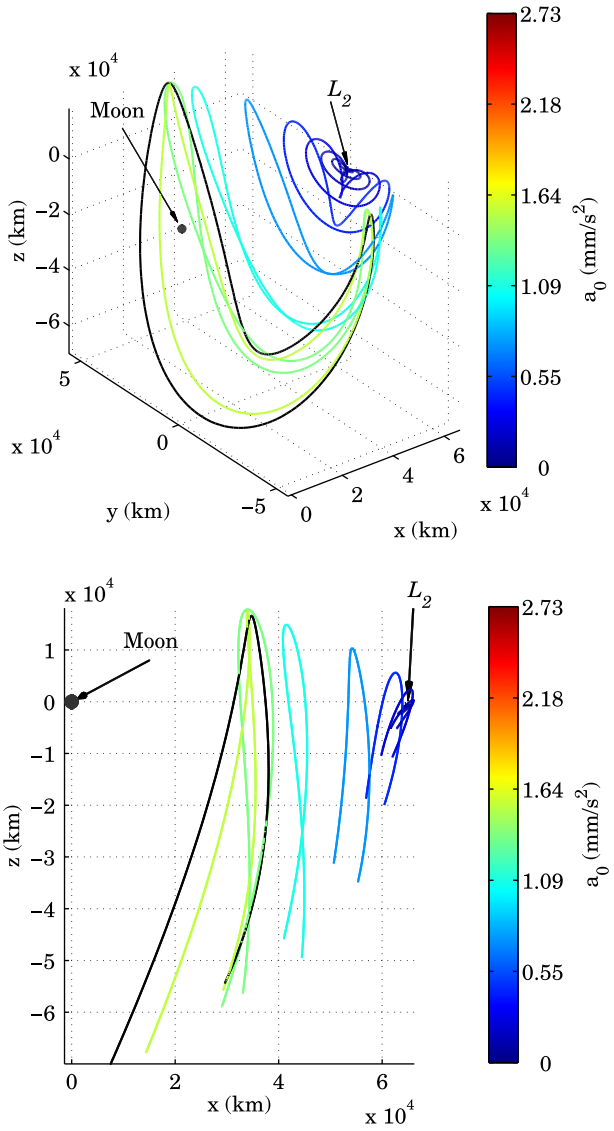

Fig. 2. A family of offset orbits in the vicinity of L_2. The Moon is plotted for scale.

as $\delta\mathbf{r} = \mathbf{r}_d - \mathbf{r}_a$, where $\mathbf{r}_d$ is the desired value of $\mathbf{r}$ and $\mathbf{r}_a$ is the actual value. Given the characteristics of this dynamical system, a periodic orbit is assumed to be symmetric across the xz plane,[2] thus, (1) the plane crossings are perpendicular, (2) the value for t_f can be set equal to the half-period, or the second crossing of the xz plane, and (3) a reduced set of variables is required for the DC process. These propositions suggest that $\{\delta y_f\ \delta\dot{x}_f\ \delta\dot{z}_f\}$ can deliver either $\{\delta x_i\ \delta\dot{y}_i\ \delta(a_0)\}$ or $\{\delta z_i\ \delta\dot{y}_i\ \delta(a_0)\}$, depending on the advantages in fixing z_i or x_i, respectively, over a set of iterations for a particular orbit. An updated state, $\{\mathbf{r}_i\ \dot{\mathbf{r}}_i\ a_0\}$, is then used to re-initialize the trajectory. The characteristic acceleration, a_0, remains constant along the orbit. The process is repeated until a convergence tolerance is met.

A family of orbits that is initialized by the linear approximation in Simo and McInnes (2010) appears in Figs. 2–5.

[2] The justification for this symmetry is described in the Appendix.

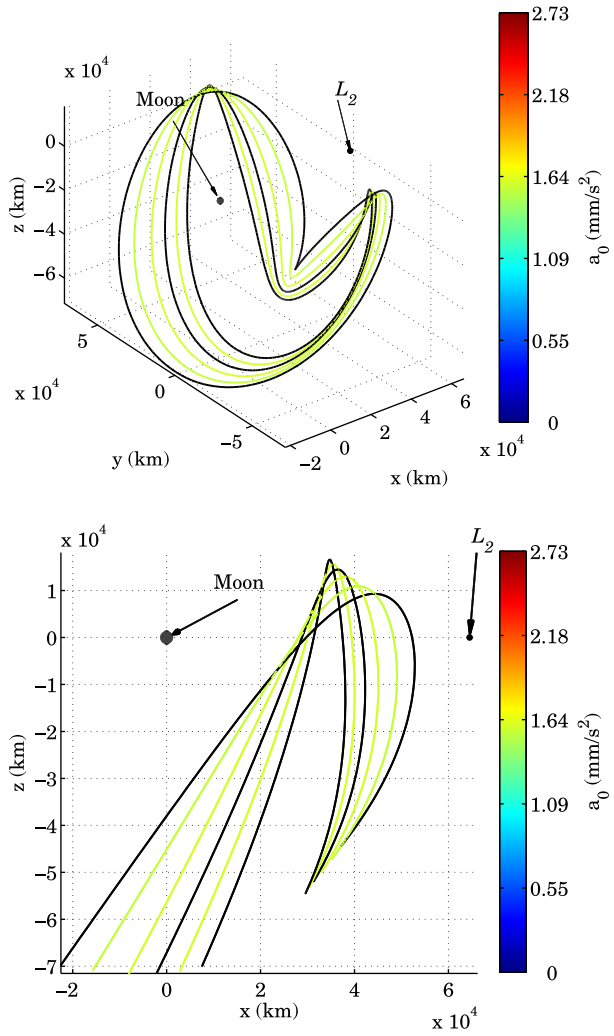

Fig. 3. A continuation of the family of orbits from the Fig. 2.

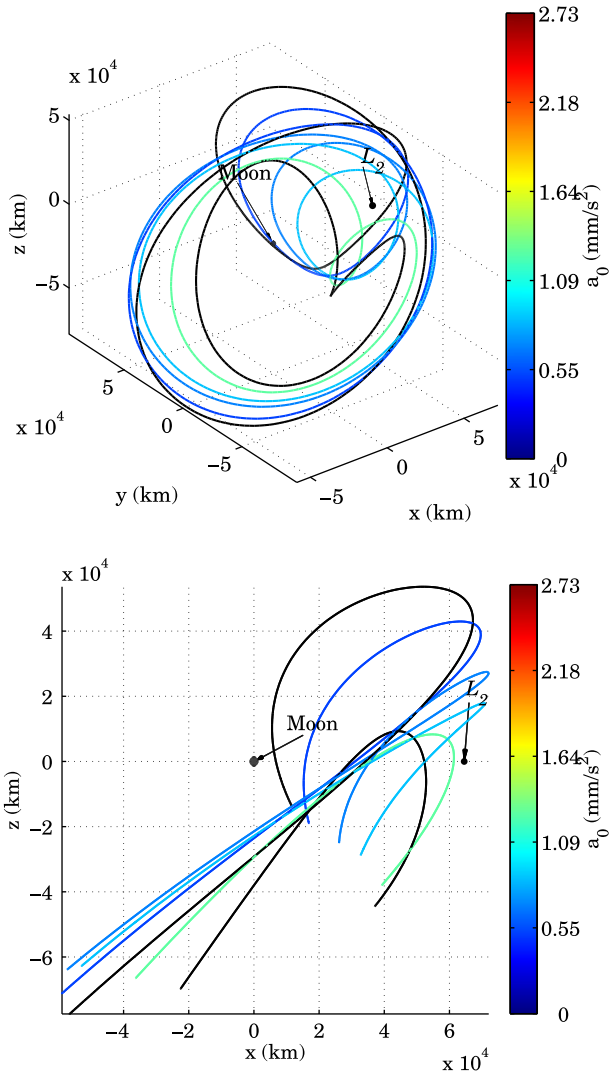

Fig. 4. A continuation of the family of orbits from the Fig. 3.

It is notable that the black orbits in Figs. 2–5 coincide with bifurcations in the eigen-structure, and possibly indicate a branching to another family of orbits. The color associated with each orbit in the figures represents the characteristic acceleration, a_0, that is required to produce the corresponding path. The final orbit of the family in Fig. 5, that is, the one with the largest amplitude in the z direction, has a characteristic acceleration of zero, indicating that it is a natural orbit. A hodograph in Fig. 6 displays the maximum z value of each orbit in the family and the corresponding x and a_0 values. Orbits corresponding to bifurcations are indicated with a large black dot. Recall that a_0 is not time-dependent and is constant along an orbit. The approximation from Simo and McInnes (2010) that is employed to initialize the DC process is successful in producing periodic orbits for initial out-of-plane distances from zero to about 300 km below the EM orbit plane (an ellipse 100 km in x and 1900 km in y). Thereafter, the continuation scheme is employed, using the initial states from the previous orbits to predict the initial state for the current orbit. At the second bifurcation (represented by the middle black orbit in Fig. 3), the continuation procedure along the family yields the orbit that require a maximum characteristic acceleration level equal to 1.6 mm/s^2. Other bifurcations along this family are also observed, indicating potential intersections with other families of solutions. The family of nonlinear orbits represented in Fig. 2 clearly does not produce trajectories with continuous communications coverage at the LSP, but demonstrates the DC process.

The accuracy of a shooting method depends on the iteration and integration tolerances, as well as the model itself. The deviations at the end of a propagation sequence are compared to iteration tolerances to determine the convergence characteristics. The preceding example employed MATLAB®'s ODE113 explicit integration routine to propagate the orbits (The MathWorks™, Inc., 2010). Default tolerances are employed, except that the relative and absolute tolerances are set to 1e−13. Compared to the ODE45 propagator, which is a single-step solver based on an explicit Runge–Kutta (4, 5) formula, the ODE113 routine is a multiple-step solver based on the Adams–Bashforth–Moulton strategy; it is also more efficient with stringent tolerances and, therefore, faster (The MathWorks™, Inc.,

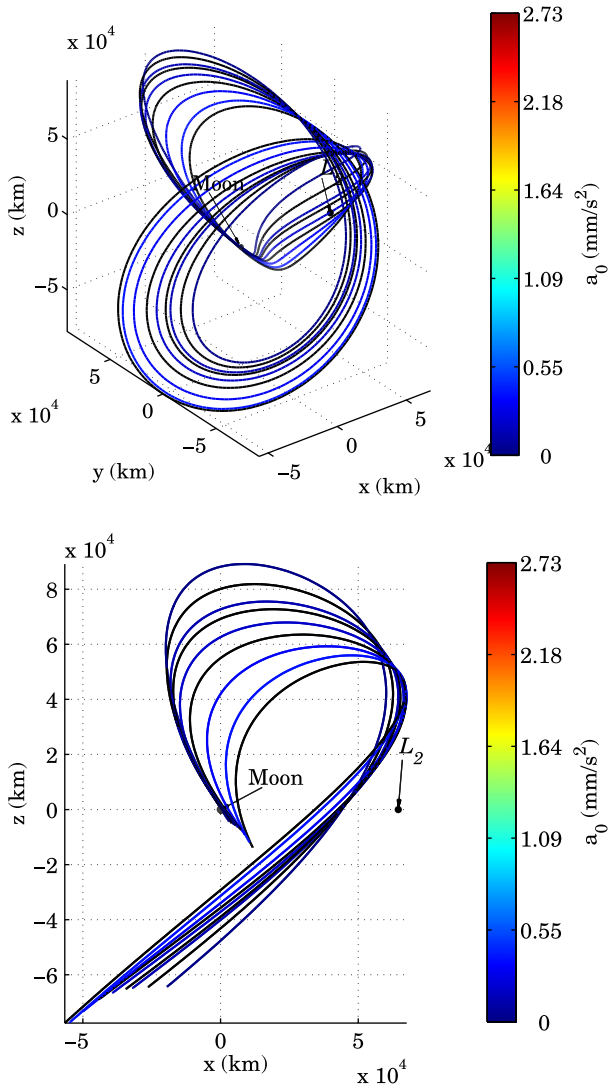

Fig. 5. A continuation of the family of orbits from the Fig. 4.

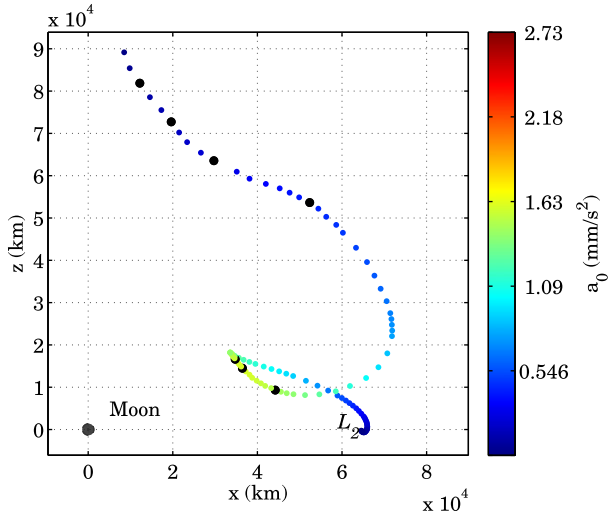

Fig. 6. A hodograph of the orbits appearing Figs. 2–5.

2010). Similar to other MATLAB® propagators, the theoretical error associated with each propagated state for the ODE113 propagator at a given step is compared to relative and absolute integration tolerances to control the step size. In reality, a propagated trajectory will diverge from a true trajectory, but the amount of divergence is reduced with tighter tolerances on the integration. Consequently, propagated trajectories are often regarded as "truth" models in mission design.

4. Finite-difference methods

Rather than computing variations relative to a reference solution, finite-difference methods (FDMs) approach the trajectory "as a whole" (Wawrzyniak and Howell, in press). A very simple guess, such as a circle or a point, is discretized into the set of vectors $\{\mathbf{r}_1,\ldots,\mathbf{r}_i,\ldots,\mathbf{r}_n\}$ at n node points (in the time domain) along the trajectory. Vector derivatives of the state vector are approximated by central differences. These approximations substitute for the true time derivatives in Eq. (1). If the initial guess for the path does not satisfy the equations of motion (usually the case), Eq. (1) will not equal zero. The goal is to force finite differences at epochs along the trajectory to equal the time derivatives in Eq. (1). Other constraints, such as periodicity, the magnitude of the unitary control direction ($\|\mathbf{u}_i\| = 1$), and path constraints (elevation, altitude, etc.), are formulated as equality constraints and are functions of the discretized path coordinates (all $\mathbf{r}_i$), control vector (all $\mathbf{u}_i$), and slack variables (all $\boldsymbol{\eta}_i$, which convert inequality path constraints into equality constraints) at each node. Converting inequality constraints to equality constraints via slack variables is an effective, straightforward strategy for dealing with inequality constraints and is adapted from linear programming (Ozimek et al., 2009; Betts, 2001). A Newton–Raphson iteration procedure is used to solve for the complete set of $\mathbf{r}_i$, $\mathbf{u}_i$, and $\boldsymbol{\eta}_i$ that satisfy Eq. (1).

The advantage of FDMs is their simplicity in terms of understanding and implementation, especially with time-dependent control profiles. The disadvantage is that the local accuracy is limited to $\mathcal{O}(\Delta t^2)$ as $\Delta t \to 0$, or the number of nodes, n, grows. The number of equations to be solved and the integration round-off error increase as n gets larger. Sample FDM solutions appear in Fig. 7. These orbits are generated with a minimum elevation constraint angle of 15° as viewed from the LSP. The Moon is to scale; $L_{1,2}$ appear as black dots. In this frame, the Sun moves in a clockwise fashion about the z axis. The initial time is defined when the Sun is along the x axis on the L_1 side of the Moon (in the direction of the Earth). At the initial time, the spacecraft are on the L_2 side of the Moon in their respective orbits, and also in the xz plane.

State vectors that are extracted at a specific epoch and then simply propagated forward from these numerical solutions eventually diverge, in part, because of dynamical and numerical sensitivities, as well as the fact that the control history, $\mathbf{u}(t)$, and the initial state do not satisfy Eq. (1) exactly, in

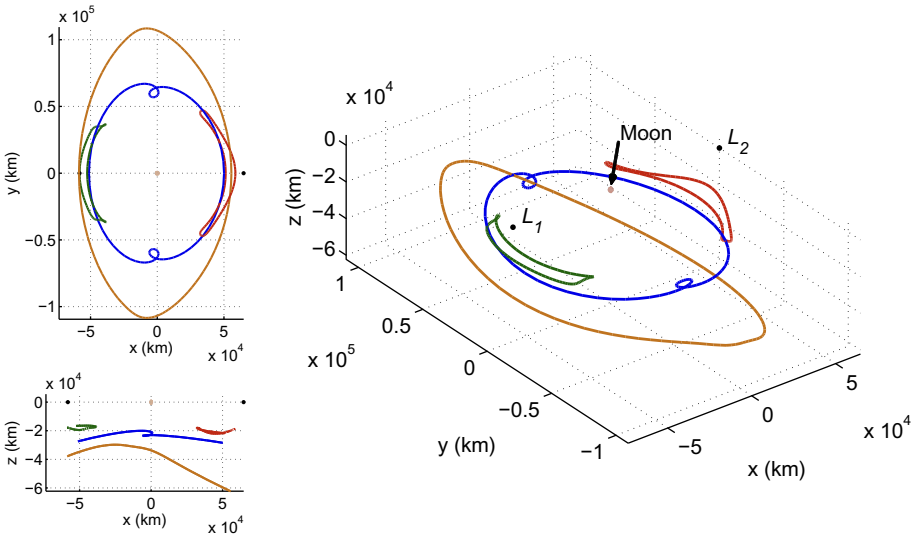

Fig. 7. Three views of four sample orbits generated by FDMs.

that solutions are accurate to $\mathcal{O}(\Delta t^2)$. However, the trajectory approximated with a FDM can potentially be used to initialize a more accurate numerical technique. Another possibility is that an FDM solution is sufficiently accurate such that small adjustments to the states and control can produce a more accurate solution or small adjustments solely to the control will allow tracking of a specified solution as a reference (Wawrzyniak and Howell, 2010). In any case, the design space for this problem is not well understood, so a trajectory that solves the equations of motion to within a small error is meaningful. If the goal is a general understanding of the design space, accomplished in a relatively quick analysis, then results from a FDM approximation can stand alone and be very insightful.

5. Collocation

Similar to FDMs, a collocation scheme also discretizes both the trajectory and control, and then delivers a solution for the discretized states simultaneously. Collocation involves minimization of the difference between the derivative of a continuous approximating polynomial and the derivative from the equations of motion at an intermediate, or defect, point (or points) on an arc between nodes along the path. While the accuracy of FDMs is limited to the step size between nodes, collocation offers more accuracy by employing higher-degree polynomials (Herman and Conway, 1996).

Because of their relative insensitivity to a poor initial guess and relative accuracy when compared to other approaches, collocation methods are increasingly common for solving BVPs, including optimal control problems. Optimization software packages such as DIDO (Ross and Fahroo, 2002) and GPOPS (Rao et al., 2008, 2010), as well as MATLAB®'s BVP*C functions (* = 4, 5, 6) (The MathWorks™, Inc., 2010; Hale et al., 2008), rely on collocation. The type of polynomial and the integration rules vary for different accuracies. Nassiri et al. (2005) employ a technique that relies on a Hermite interpolating polynomial and Simpson quadrature rules (a.k.a., Hermite–Simpson collocation), which possess a local accuracy of $\mathcal{O}(\Delta t^5)$, to minimize the time of flight along a solar sail interplanetary transfer. Ozimek et al. (2009) demonstrate: (1) a Hermite–Simpson collocation scheme for a solar sail in the EM system, and (2) a highly accurate method for application in the same system that is based on a seventh-degree polynomial subject to Gauss–Lobatto integration constraints with a local accuracy of $\mathcal{O}(\Delta t^{12})$; both methods in Ozimek et al. (2009) employ equally spaced nodes. In Ozimek et al. (2010), mesh refinement is employed in the seventh-degree Gauss–Lobatto process, strategically redistributing and reducing the number of nodes required for a solution of equal accuracy across all nodes.

Employing the Hermite–Simpson collocation scheme[3] described in Ozimek et al. (2009) and the same initial guesses that are used to generate the orbits via finite-difference methods discussed previously, trajectories similar to those appearing in Fig. 7 emerge. The orbits generated by the Hermite–Simpson collocation scheme appear in Fig. 8. The only visible difference in the four periodic orbits is the shape of the "twists" along the y axis in the blue trajectory. Near these twists, the two blue orbits differ by approximately 10,000 km. Likewise, the gold orbits differ by approximately 1700 km, the green by approximately 2600 km, and the red by almost 3000 km. These differences are small when one considers that the initial guess for each pair of orbits is either a luni-axial circle (for those orbits centered below the Moon) or a stationary point (for the orbits offset below the Lagrange points) and generally not similar to the resulting

[3] With the exception of partial derivatives derived via central difference approximations.

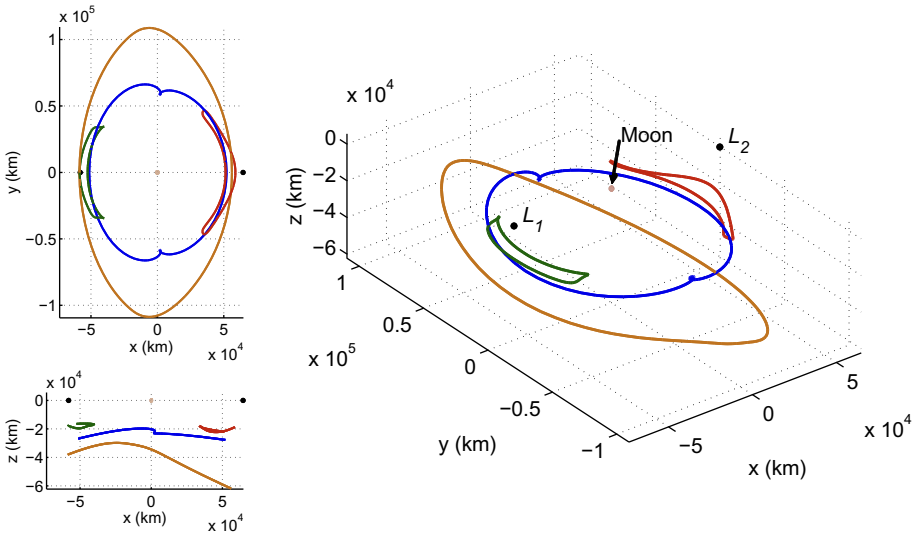

Fig. 8. Three views of four example orbits generated by a Hermite–Simpson collocation method.

solutions. Nevertheless, both the FDM and the collocation strategies result in orbits that nearly—that is, do not exactly—solve the equations of motion.

Similar to FDMs, collocation returns the required control history, $\mathbf{u}(t)$, as well as a finite set of states along the trajectory. Unlike the FDM, if a trajectory is developed using a higher-accuracy collocation scheme, direct numerical integration process initiated by extracting a set of these states, along with the specified control history, often results in a solution that resembles the original collocation solution. However, this observation in no way implies that solutions from one numerical approach are superior to those emerging from another method. Each periodic orbit generated here can serve as a reference trajectory for mission design, depending the phase of mission design as well as on the necessary level of accuracy required from the generating numerical method and accuracy of the dynamical model. Naturally, navigation and flight-path control must be considered for an actual flight as model uncertainties and mis-modeling result in an actual trajectory that diverges from any reference.

6. Bootstrapping: sequential numerical methods

The orbits generated by the any of the numerical strategies described in this summary *nearly* solve Eq. (1). These reference orbits are of varying accuracy, and, if a sailcraft is flown along one of these orbits, its actual path would diverge from the reference path. Furthermore, an explicit integration of position and velocity states, along with a complete control history, from a solution generated by any numerical procedure, especially a lower-accuracy method like the FDM, will diverge from the reference path. Mission designers can respond to these accuracy issues using various options. One possibility is to simply design a controller to maintain the reference path, either by incorporating an additional form of control (Simo and McInnes, 2010) or via small adjustments to the control profile (Wawrzyniak and Howell, 2010); either control technique may yield an infeasible trajectory without additional processing, however. Another option is to improve the reference trajectory from a lower-accuracy method by using that less-accurate solution to seed a higher-accuracy process. This sequential procedure is not always successful, and trajectories resulting from higher-accuracy solutions still require controllers to maintain the reference path. However, the new solutions may result in a better understanding of the design space.

One approach to improve a reference trajectory is to use a solution generated by the FDM algorithm to seed a collocation process. Each of the four sample FDM orbits from Fig. 7 is used to initialize a Hermite–Simpson collocation scheme. The collocation process converges quickly on new solutions with nearly identical control histories; the maximum isochronous difference in position along the path for each updated trajectory is approximately 100 km.

Another approach to refining a lower-accuracy FDM solution is to use it to seed a multiple-shooting scheme. In Fig. 9, the initial states from the blue orbit in Fig. 7 are corrected via a multiple-shooting algorithm. In multiple shooting, the trajectory is decomposed into segments and corrected such that the segment end points coincide. Deviations at the end of the shorter arc segments in multiple-shooting algorithms are generally smaller than if the trajectory is propagated to the next plane crossing, as is the case with single shooting. Smaller deviations are easier to correct, thus, multiple-shooting algorithms tend to be more numerically stable than single-shooting processes. The black path in Fig. 9 represents a trajectory propagated from four points (represented by asterisks) along the FDM reference orbit (in blue). Multiple shooting is employed to enforce continuity at the end points of the black subarcs. The red path is the propagated trajectory that results after convergence given an initial guess from

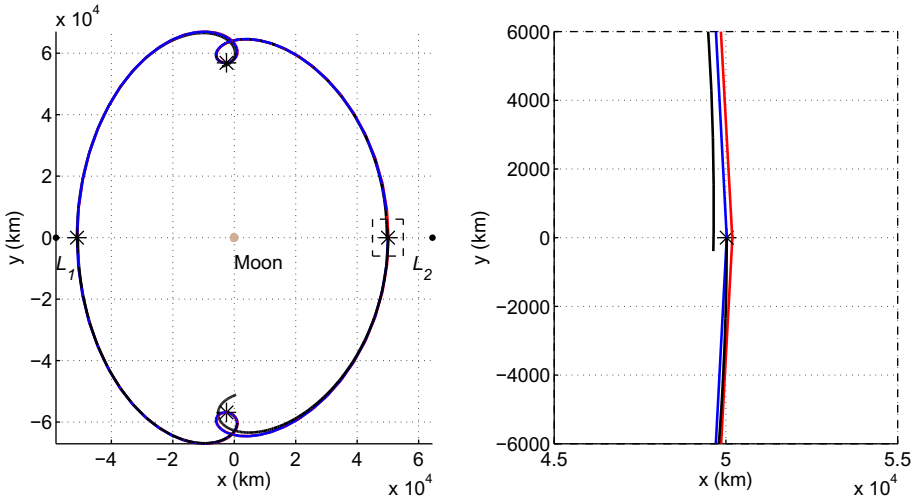

(a) Full view (b) Zoom near L_2

Fig. 9. A FDM-generated reference orbit (blue), four segments in a multiple-shooting scheme (black), and a continuous path resulting from multiple shooting (red). (For interpretation of the references to colour in this figure legend, the reader is referred to the web version of this article.)

the FDM solution for the state vectors and control histories. In the figure, all motion is clockwise, originating near the L_2 point. The blue FDM path is periodic because a periodicity constraint is imposed in the FDM algorithm. The red path, generated via multiple shooting, is close to, but not exactly, periodic, as its endpoints near L_2 differ in position by appoximately 100 km. Continuity is not enforced at the end of the final arc and the beginning of the first arc in the multiple-shooting approach because the equations are not independent, leading to difficulties in convergence of the solution. Additionally, the control history, which is *not* corrected with the states, does not accurately solve the EOMs. While not investigated here, with additional complexity in the algorithm, shooting might also be used to correct the control history.

7. Conclusions

The numerical methods described here are useful tools for uncovering solar sail trajectories in complex dynamical regimes and for correcting trajectories developed analytically. These techniques complement analytical approaches and approximations. Lower-accuracy results may sometimes initialize higher-accuracy solutions. Additionally, since the numerical solutions nearly solve the equations of motion, some form of adjustment to the control might be employed to complete a periodic solution or meet other trajectory goals; future efforts will address this issue. Numerical methods are important tools for solar sail mission designers.

Acknowledgements

The authors would like to thank Chris Patterson for his help with extending the Mirror Theorem to this solar sail application. Dan Grebow and Martin Ozimek are also acknowledged for their insightful suggestions.

Appendix A. Symmetry in solar sail trajectories

It is well known that certain symmetries exist in the circular restricted three-body problem (CR3BP). One such symmetry arises from the time-invariance, or reversibility, of the equations of motion. The equations of motion for the CR3BP are

$$\ddot{x} - 2\dot{y} - x + \frac{(1-\mu)(x+\mu)}{r_1^3} + \frac{\mu(x-1+\mu)}{r_2^3} = 0 \tag{A.1}$$

$$\ddot{y} + 2\dot{x} - y + \frac{(1-\mu)y}{r_1^3} + \frac{\mu y}{r_2^3} = 0 \tag{A.2}$$

$$\ddot{z} + \frac{(1-\mu)z}{r_1^3} + \frac{\mu z}{r_2^3} = 0 \tag{A.3}$$

If trajectories are reversed across the xz plane, then

$$x \to x, \quad y \to -y, \quad z \to z, \quad t \to -t$$

The subsequent path derivatives are

$$\frac{d(x)}{d(-t)} = -\dot{x}, \quad \frac{d(-y)}{d(-t)} = \dot{y}, \quad \frac{d(z)}{d(-t)} = -\dot{z}$$
$$\frac{d(-\dot{x})}{d(-t)} = \ddot{x}, \quad \frac{d(\dot{y})}{d(-t)} = -\ddot{y}, \quad \frac{d(-\dot{z})}{d(-t)} = \ddot{z}$$

If these states are substituted into Eqs. (A.1)–(A.3), the same equations of motion as those appearing in Eqs. (A.1)–(A.3) are recovered. The advantage of this phenomenon is that a *mirror configuration* occurs at the crossing of the xz plane or the y axis (Roy and Ovenden, 1955). Two possible mirror configurations are possible: (P) when all point masses (i.e., the primaries and the spacecraft) lie in a plane and all velocity vectors are at right angles to that plane and (A) when all point masses lie along an axis

and all velocity vectors are at right angles to that axis, but not necessarily parallel to each other. Orbits are periodic if, at two separate epochs, a mirror configuration occurs (Roy and Ovenden, 1955). An example of a periodic orbit with two mirror configurations in an arbitrary CR3B system appears in Fig. A.1. Because of the mirror configurations, certain states can be assumed to be zero at the perpendicular crossings of the symmetry plane (or axis). The implication of these assumptions is that a trajectory only requires numerical integration from one mirror configuration to the subsequent mirror configuration, or one half-period, to determine a symmetric periodic orbit.

For a solar sail in the Earth–Moon CR3B system, a similar symmetry occurs in the time reversal of the equations of motion. To begin, **u** from Eq. (1) is represented in terms of a Sun-fixed frame (McInnes, 1999), that is,

$$\mathbf{u} = \cos\alpha\hat{\ell}_1 + \sin\alpha\cos\delta\hat{\ell}_2 + \sin\alpha\sin\delta\hat{\ell}_3 \tag{A.4}$$

where $\{\hat{\ell}_1, \hat{\ell}_2, \hat{\ell}_3\}$ are the three components of the sunlight vector. When expressed in the EM rotating frame, the equations of motion for a solar sail spacecraft are

$$\ddot{x} - 2\dot{y} - x + \frac{(1-\mu)(x+\mu)}{r_1^3} + \frac{\mu(x-1+\mu)}{r_2^3} = \beta(\mathrm{c}_{\Omega t}\mathrm{c}_\alpha^3 + \mathrm{s}_{\Omega t}\mathrm{s}_\alpha\mathrm{c}_\alpha^2\mathrm{s}_\delta) \tag{A.5}$$

$$\ddot{y} + 2\dot{x} - y + \frac{(1-\mu)y}{r_1^3} + \frac{\mu y}{r_2^3} = \beta(-\mathrm{s}_{\Omega t}\mathrm{c}_\alpha^3 + \mathrm{c}_{\Omega t}\mathrm{s}_\alpha\mathrm{c}_\alpha^2\mathrm{s}_\delta) \tag{A.6}$$

$$\ddot{z} + \frac{(1-\mu)z}{r_1^3} + \frac{\mu z}{r_2^3} = \beta(\mathrm{s}_\alpha\mathrm{c}_\alpha^2\mathrm{c}_\delta) \tag{A.7}$$

where $\mathrm{c} \equiv \cos$, $\mathrm{s} \equiv \sin$, and $\beta = a_0/a^*$. When these equations are time reversed, the following equations result

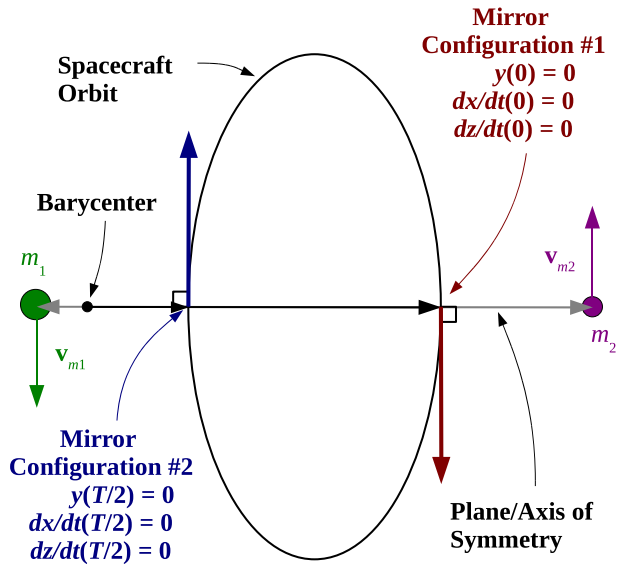

Fig. A.1. An example of a mirror configuration (either P-type or A-type).

$$\ddot{x} - 2\dot{y} - x + \frac{(1-\mu)(x+\mu)}{r_1^3} + \frac{\mu(x-1+\mu)}{r_2^3} = \beta(\mathrm{c}_{\Omega t}\mathrm{c}_\alpha^3 - \mathrm{s}_{\Omega t}\mathrm{s}_\alpha\mathrm{c}_\alpha^2\mathrm{s}_\delta) \tag{A.8}$$

$$\ddot{y} + 2\dot{x} - y + \frac{(1-\mu)y}{r_1^3} + \frac{\mu y}{r_2^3} = \beta(-\mathrm{s}_{\Omega t}\mathrm{c}_\alpha^3 - \mathrm{c}_{\Omega t}\mathrm{s}_\alpha\mathrm{c}_\alpha^2\mathrm{s}_\delta) \tag{A.9}$$

$$\ddot{z} + \frac{(1-\mu)z}{r_1^3} + \frac{\mu z}{r_2^3} = \beta(\mathrm{s}_\alpha\mathrm{c}_\alpha^2\mathrm{c}_\delta) \tag{A.10}$$

Note the sign differences in Eqs. (A.5) and (A.8) and Eqs. (A.6) and (A.9). Time invariance is only possible for solar sails in the EM system if $\delta = 0, 180°$ at the time of the mirror configuration. This property is also observed and employed by Farrés et al. (2010). While Roy and Ovenden (1955) specify that the "*n*-point masses are acted upon by their mutual gravitational forces only" the Mirror Theorem still holds for the case of a solar sail in the EM system because the Sun is in a plane containing the Earth, Moon, and sailcraft at the times of the sailcraft crossing of that plane. Although solar gravity is not modeled, solar radiation pressure acts in a manner similar to gravity, albeit repulsive, in this system.

References

Andreu, M.A. The Quasi-Bicircular Problem. Ph.D. Thesis, Universitat de Barcelona, Barcelona, Spain, 1998.

Betts, J.T. Survey of numerical methods for trajectory optimization. Journal of Guidance, Control, and Dynamics 22 (2), 193–207, 1998.

Betts, J.T. Practical Methods for Optimal Control Using Nonlinear Programming. SIAM, Philadelphia, Pennsylvania, 2001.

Farquhar, R.W., Kamel, A.A. Quasi-periodic orbits about the translunar libration point. Celestial Mechanics 7, 458–473, 1970.

Farrés, A., Jorba, À. Periodic and quasi-periodic motions of a solar sail close to SL_1 in the Earth–Sun system. Celestial Mechanics and Dynamical Astronomy 107 (1–2), 233–253, doi:10.1007/s10569-010-9268-4, 2010.

Grebow, D.J., Ozimek, M.T., Howell, K.C. Advanced modeling of optimal low-thrust pole-sitter trajectories. Acta Astronautica 67 (7–8), 991–1001, 2010.

Guzmán, J.J. Spacecraft Trajectory Design in the Context of a Coherent Restricted Four-Body Problem. Ph.D. Thesis, Purdue University, West Lafayette, Indiana, 2001.

Hale, N., Moore, D.R. A sixth-order extension to the MATLAB package bvp4c of J. Kierzenka and L. Shampine. Tech. Rep. 08/04, Oxford University Computing Laboratory, Numerical Analysis Group, Oxford, 2008.

Herman, A.L., Conway, B.A. Direct optimization using collocation based on high-order Gauss–Lobatto quadrature rules. Journal of Guidance, Control, and Dynamics 19 (3), 592–599, 1996.

Howell, K.C., Pernicka, H.J. Numerical determination of Lissajous trajectories in the restricted three-body problem. Celestial Mechanics 41 (1–4), 107–124, 1988.

Julier, S.J., Uhlmann, J.K., Durrant-Whyte, H.F. A new approach for filtering nonlinear systems. In: American Control Conference. Seattle, Washington, paper No. 5058100, 1995.

McInnes, A.I.S. Strategies for Solar Sail Mission Design in the Circular Restricted Three-Body Problem. M.S. Thesis, Purdue University, West Lafayette, Indiana, 2000.

McInnes, C.R.. Solar Sailing: Technology, Dynamics and Mission Applications. Space Science and Technology. Springer-Praxis, New York, 1999.

McInnes, C.R., McDonald, A.J.C., Simmons, J.F.L., MacDonald, E.W. Solar sail parking in restricted three-body systems. Journal of Guidance, Control, and Dynamics 17 (2), 399–406, 1994.

Nassiri, N., Mehdizadeh, N., Jalali, M. Interplanetary flight using solar sails. In: RAST 2005. 2nd International Conference on Recent Advances in Space Technologies. Istanbul, Turkey, pp. 330–334, 2005.

Nuss, J.S. The Use of Solar Sails in the Circular Restricted Problem of Three Bodies. M.S. Thesis, Purdue University, West Lafayette, Indiana, 1998.

Ozimek, M.T., Grebow, D.J., Howell, K.C. Design of solar sail trajectories with applications to lunar south pole coverage. Journal of Guidance, Control, and Dynamics 32 (6), 1884–1897, 2009.

Ozimek, M.T., Grebow, D.J., Howell, K.C. A collocation approach for computing solar sail lunar pole-sitter orbits. The Open Aerospace Engineering Journal 3, 65–75, 2010.

Rao, A.V. A survey of numerical methods for trajectory optimization. In: AAS/AIAA Astrodynamics Specialists Conference. Pittsburgh, Pennsylvania, paper No. AAS 09-334, 2009.

Rao, A.V., Benson, D.A., Darby, C.L., Patterson, M.A., Francolin, C., Huntington, G.T. Algorithm 902: GPOPS, a MATLAB software for solving multiple-phase optimal control problems using the Gauss pseudospectral method. ACM Transactions on Mathematical Software 37 (2), 1–39, 2010.

Rao, A.V., Benson, D.A., Huntington, G.T., Francolin, C., Darby, C.L., M.A. Patterson, M.A. User's manual for GPOPS: A MATLAB package for dynamic optimization using the Gauss pseudospectral method. Tech. rep., University of Florida, Naval Postgraduate School, Monterey, CA, 2008.

Ross, I.M., Fahroo, F. User's manual for DIDO 2002: A MATLAB package for dynamic optimization. Tech. Rep. AA-02-002, Department of Aeronautics and Astronautics, Naval Postgraduate School Technical Report, Naval Postgraduate School, Monterey, CA, 2002.

Roy, A.E., Ovenden, M.W. On the occurrence of commensurable mean motions in the solar system: II. The mirror theorem. Monthly Notices of the Royal Astronomical Society 115 (3), 296–309, 1955.

Sengupta, P., Vadali, S.R., Alfriend, K.T. Second-order state transition for relative motion near perturbed, elliptic orbits. Celestial Mechanics and Dynamical Astronomy 97, 101–129, doi:10.1007/s10569-006-9054-5, 2007.

Simo, J., McInnes, C. Designing displaced lunar orbits using low-thrust propulsion. Journal of Guidance, Control, and Dynamics 33 (1), 259–265, 2010.

Stoer, J., Bulirsch, R. Introduction to Numerical Analysis, 3rd ed Springer-Verlag, New York, 2002.

The MathWorks™, Inc. MATLAB®, Version 7.11.0 (R2010b). Natick, Massachusetts, <www.mathworks.com>, 2010.

Waters, T.J., McInnes, C.R. Periodic orbits above the ecliptic in the solar-sail restricted three-body problem. Journal of Guidance, Control, and Dynamics 30 (3), 687–693, 2007.

Wawrzyniak, G.G., Howell, K.C. Trajectory control for a solar sail spacecraft in an offset lunar orbit. In: 61st International Astronautical Congress. Prague, Czech Republic, paper No. IAC-10.C1.2.3, 2010.

Wawrzyniak, G.G., and Howell, K.C. Generating solar sail trajectories in the Earth-Moon system using augmented finite-difference methods," International Journal of Aerospace Engineering, vol. 2011, Article ID 476197, 2011. doi:10.1155/2011/476197.